XIV International Conference on Computational Plasticity. Fundamentals and Applications
COMPLAS 2017
E. Oñate, D.R.J. Owen, D. Peric and M. Chiumenti (Eds)

THREE-DIMENSIONAL NUMERICAL ANALYSIS OF ROTARY PIERCING PROCESS

KOJI YAMANE†, KAZUHIRO SHIMODA† AND AKIHITO YAMANE†

† Research and Development, Process Research Laboratories
Nippon Steel and Sumitomo Metal Corporation
1-8 Fuso-Cho, Amagasaki, Hyogo, 660-0891, Japan
e-mail: yamane.6nq.kohji@jp.nssmc.com

Key words: Rotary Piercing, Seamless Tube, FEM, Toe Angle, Feed Angle, Shear Strain.

Abstract. Three-dimensional numerical analysis of the rotary piercing process was performed by the rigid plastic finite element method. Rotary piercing, also known as the Mannesmann piercing process, is a hot rolling process that manufactures seamless tubes. In this process, the heated round billet is rotated by the rolls and pierced by the plug as an internal tool. Numerical analysis was conducted to investigate the deformation behaviour during rotary piercing and redundant shear deformation specific to this process. This paper discusses the effect of various rolling parameters on redundant shear deformation.

1 INTRODUCTION

The rotary piercing process is one method for manufacturing seamless tubes that are used for oil country tubular goods and so forth. It is also known as the Mannesmann piercing process, the concept of which was invented by the Mannesmann brothers in Germany in 1886. More than 100 years later, a cone-type piercing mill with a high toe angle was developed by Sumitomo Metal Industries, Ltd. In this process, the heated round billet is rolled by a pair of rolls and held by a pair of guide rolls. The axes of the rolls are inclined opposite to each other in order to advance the round billet. The round billet is rotated by the rolls and pierced by the plug as an internal tool. While the round billet is rotated helically, the wall thickness is reduced by rolling with the rolls and the plug. As previously described, the tube is subject to large deformation in this process. Moreover, little study has been done concerning complex boundary conditions in this process: the round billet has a free surface, the billet-roll contact area is narrow, and the direction of the friction forces affecting the billet-roll contact surface often changes. It was thus difficult to model the numerical analysis of the rotary piercing process. Therefore, the boundary conditions were investigated in a hot rolling experiment. Setting the boundary conditions that match the experimental results, the three-dimensional numerical analysis model of the rotary piercing process was developed by the rigid plastic finite element method in 2006. The developed numerical analysis was undertaken in order to investigate the deformation behaviour during rotary piercing and redundant shear deformation specific to this process. Such redundant shear deformation is considered to be one of the parameters that may cause propagation defects on the internal surface of the tube. This paper puts its focus on the effect of various rolling parameters on redundant shear deformation.

2 NUMERICAL ANALYSIS MODEL

Three-dimensional deformation analysis was performed by the rigid plastic finite element method using DEFORM-3D. The numerical analysis model of the rotary piercing process is shown in **Fig. 1**. The rolls rotate in the same direction with a constant rotational velocity of 60 rpm, the disc guide rolls rotate in the opposite directions with a constant rotational velocity of 4.0 rpm, and the plug is rotated by the rolled billet. All the tools were modeled as rigid bodies, the billet was modeled as Lagrange tetrahedral elements, the billet material was carbon steel C45, and the billet temperature was 1200°C. This numerical analysis assumed a mechanical calculation scheme. To investigate the boundary conditions, the deformation behavior of the tube was analyzed in the hot rolling experiment. This experimental results showed that the circumferential velocity of the rolled material was slightly lower than that of the roll. Since hardly any metal relative to the roll slipped, the friction model of the roll was approximated to sticking. Assuming that the friction model depends on the metal slipping velocity relative to the tool, the shear friction coefficient m for the roll was set to 1.0.

In the hot rolling experiment and the developed numerical analysis, the toe angle γ and the feed angle β were varied. The toe angle γ is the opening angle of the roll axis with respect to the pass line. As shown in **Fig. 2**, the roll diameter varies depending on the toe angle γ to keep the roll face angle α constant. **Figure 3** shows the feed angle β that is the inclination angle of the roll axis with respect to the pass line. As the feed angle β is increased, the advance direction velocity of the rolled material increases.

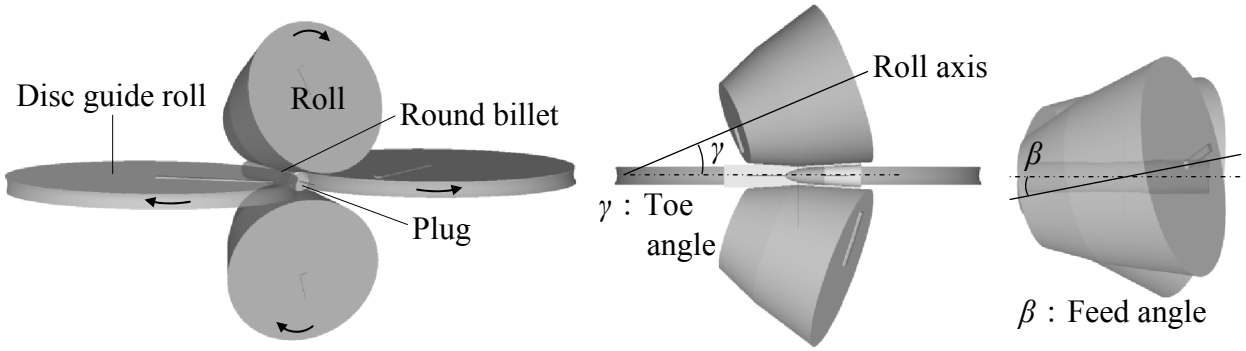

Figure 1: Numerical analysis model of the rotary piercing process.

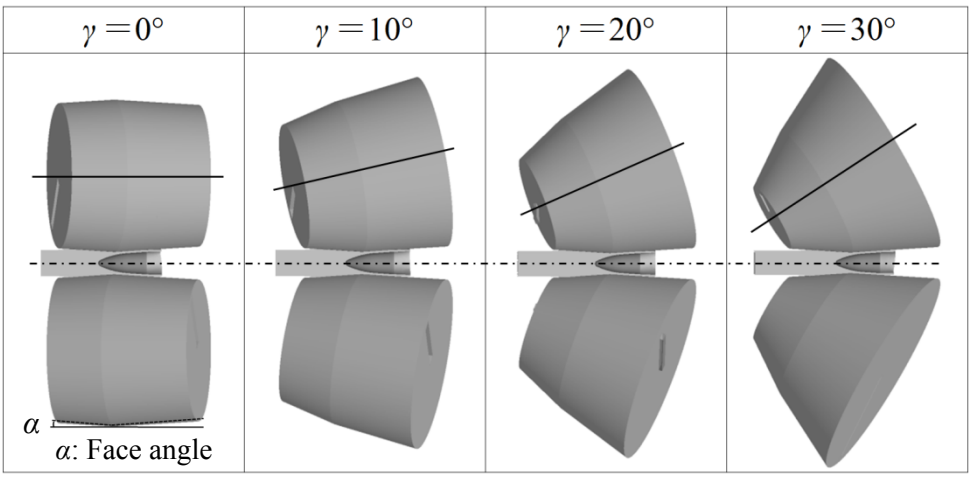

Figure 2: Schematic of the toe angle γ (at the feed angle β = 10°).

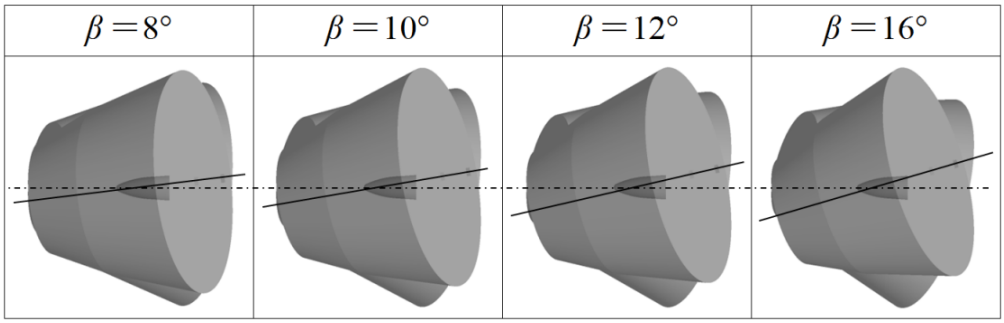

Figure 3: Schematic of the feed angle β (at the toe angle $\gamma = 20°$).

3 NUMERICAL ANALYSIS MODEL VALIDATION

3.1 Dimensional accuracy

To validate the developed numerical analysis model, the dimensions of the tube in the numerical analysis were compared with those of the hot rolling experiment. **Figure 4** shows both the longitudinal and transverse sections of the semi-finished product. The upper part shows the experimental results and the lower part shows the numerical analysis results. The numerical analysis results agree with the experimental results concerning the shape of the semi-finished product. As shown in **Fig. 5**, the difference in the circumferential length of the semi-finished product between the experiment and the numerical analysis was less than 2%.

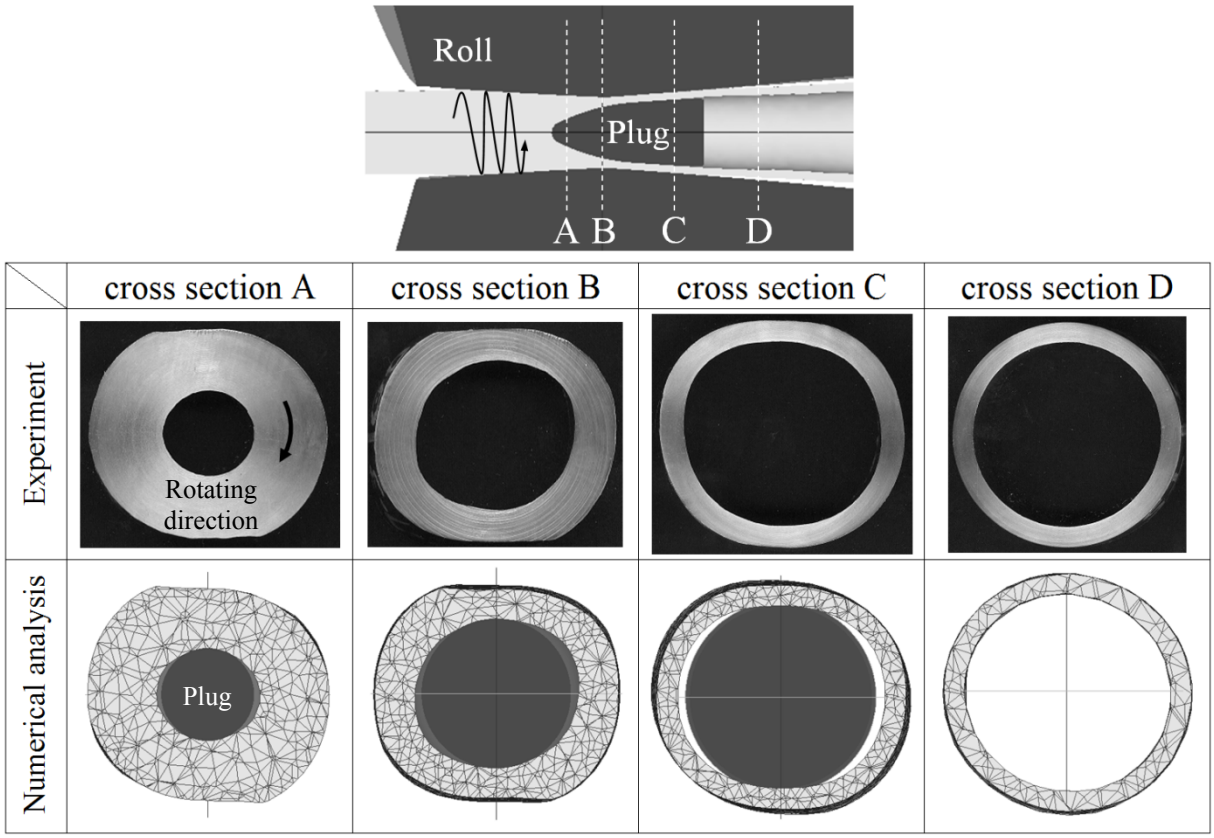

Figure 4: Shape of the semi-finished product during rotary piercing.

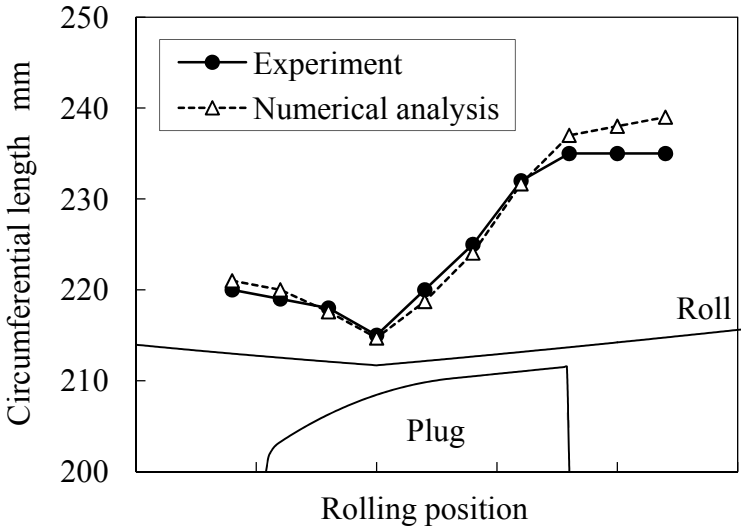

Figure 5: Comparison of the circumferential length of the semi-finished product between the experiment and the numerical analysis.

3.2 Circumferential shear deformation

In the rotary piercing process, the external surface of the rolled material follows the roll, whereas its internal surface follows the plug. Since the external surface velocity is larger than the internal surface velocity, the circumferential velocity difference between the external surface of the rolled material and its internal surface is generated. As a result, redundant shear deformation occurs in the circumferential direction when the round billet is rolled by the rolls and the plug. The measurement of circumferential shear strain $\gamma_{r\theta}$ is illustrated in **Fig. 6**. In the experiment, the twist angle θ in the circumferential direction was investigated by rolling a billet filled with Kanthal wire. In the numerical analysis, the twist angle θ in the circumferential direction was investigated by measuring the material flow in the rolling cross section. **Figure 7** shows the comparison of the twist angle θ in the circumferential direction between the experiment and the numerical analysis in each rolling cross section. The twist angle θ in the experiment was 30° and the twist angle θ in the numerical analysis was 32°. The developed numerical analysis results show agreement with the experimental results concerning circumferential shear strain $\gamma_{r\theta}$.

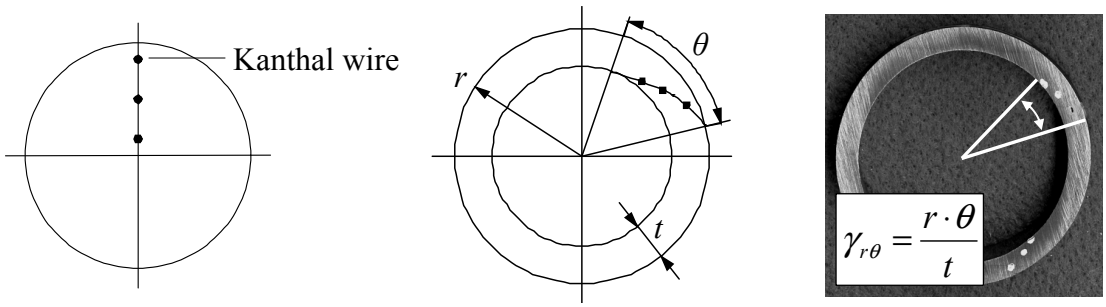

Figure 6: Measurement of circumferential shear strain $\gamma_{r\theta}$.

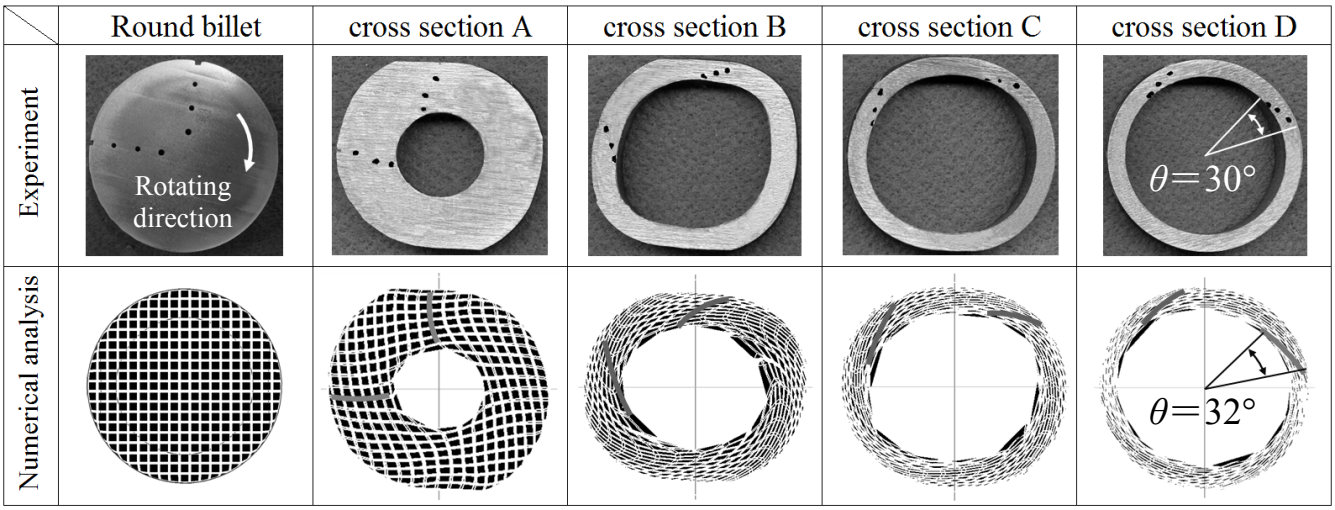

Figure 7: Comparison of the twist angle θ in the circumferential direction between the experiment and the numerical analysis.

4 RESULTS AND DISCUSSION

4.1 Effect of toe angle γ on circumferential shear strain $\gamma_{r\theta}$

Figure 8 shows the effect of the toe angle γ on circumferential shear strain $\gamma_{r\theta}$. The rolling conditions were the feed angle β = 10°, the elongation ratio (rolled length L' / billet length L) = 3.0, and the diameter expansion ratio (rolled diameter D' / billet diameter D) = 1.06. In the experiment and the numerical analysis, circumferential shear strain $\gamma_{r\theta}$ was suppressed as the toe angle γ was increased. The cause of this phenomenon was that the roll diameter varied due to the toe angle γ. As the toe angle γ is increased, the roll diameter on the inlet side is smaller. At the high toe angle, the small roll diameter on the inlet side allows a decrease in the external surface velocity of the rolled material. On the other hand, the internal surface velocity of the rolled material is affected by the plug geometry. Taking these results into account, on the inlet side of the roll, the circumferential velocity difference between the external surface of the rolled material and its internal surface decreases as the toe angle γ is increased.

Figure 9 shows the increment of the twist angle θ in the circumferential direction during rotary piercing. The numerical analysis confirmed that the twist angle θ increased on the inlet side of the roll. On the inlet side of the roll, decreasing the plug diameter led to an increase in the circumferential velocity difference of the rolled material. Reducing the wall thickness of the tube under the condition that the circumferential velocity difference of the rolled material was large, the twist angle θ increased significantly. On the outlet side of the roll, increasing the plug diameter led to a decrease in the circumferential velocity difference of the rolled material. Additionally, since the wall thickness of the tube was slightly redused, the twist angle θ hardly increased. Consequently, the twist angle θ in the toe angle γ = 0° was twice as large as the twist angle θ in the toe angle γ = 30°. It is interpreted from this study that decreasing the circumferential velocity difference of the rolled material on the inlet side of the roll due to the toe angle γ suppresses circumferential shear strain $\gamma_{r\theta}$.

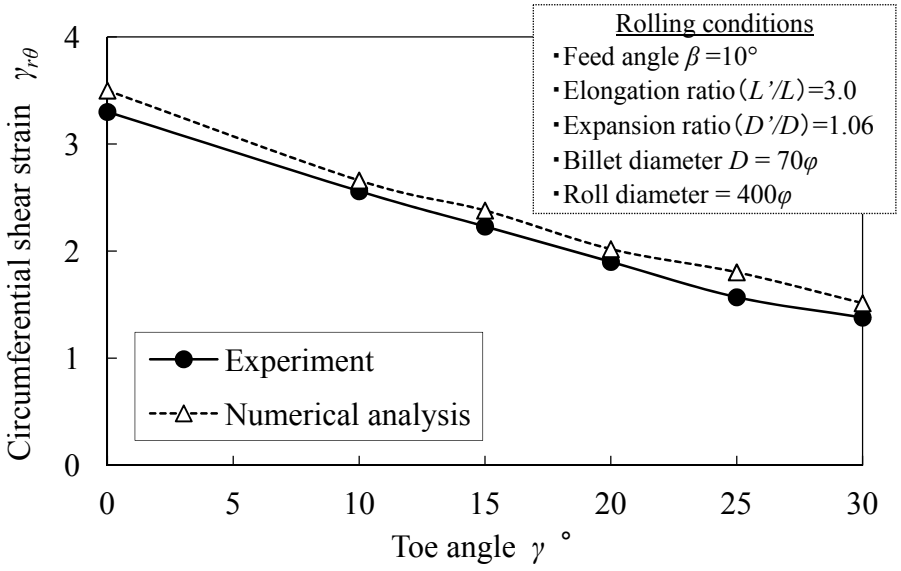

Figure 8: Effect of the toe angle γ on circumferential shear strain $\gamma_{r\theta}$.

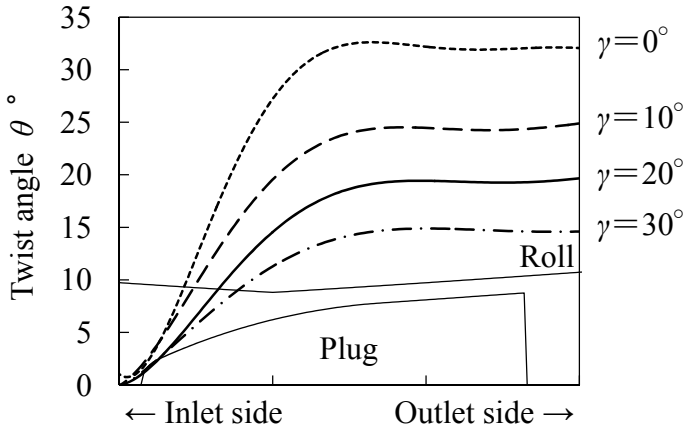

Figure 9: Increment of the twist angle θ in the circumferential direction during rotary piercing in the numerical analysis.

4.2 Effect of feed angle β on circumferential shear strain $\gamma_{r\theta}$

Figure 10 shows the effect of the feed angle β on circumferential shear strain $\gamma_{r\theta}$. The rolling conditions were the toe angle γ = 20°, the elongation ratio (rolled length L' / billet length L) = 3.0, and the diameter expansion ratio (rolled diameter D' / billet diameter D) = 1.06. In the experiment and the numerical analysis, circumferential shear strain $\gamma_{r\theta}$ was suppressed as the feed angle β was increased. This phenomenon was attributed to that the advance direction velocity of the rolled material increased in proportion to sin β. Therefore, the number of rolling times decreased as the feed angle β was increased. The effect of the feed angle β on the number of rolling times is shown in **Fig. 11**. The numerical analysis confirmed that most of circumferential shear strain $\gamma_{r\theta}$ occured when the tube was rolled by the rolls and the plug. The results from this study indicates that decreasing the number of rolling times due to the feed angle β suppresses circumferential shear strain $\gamma_{r\theta}$.

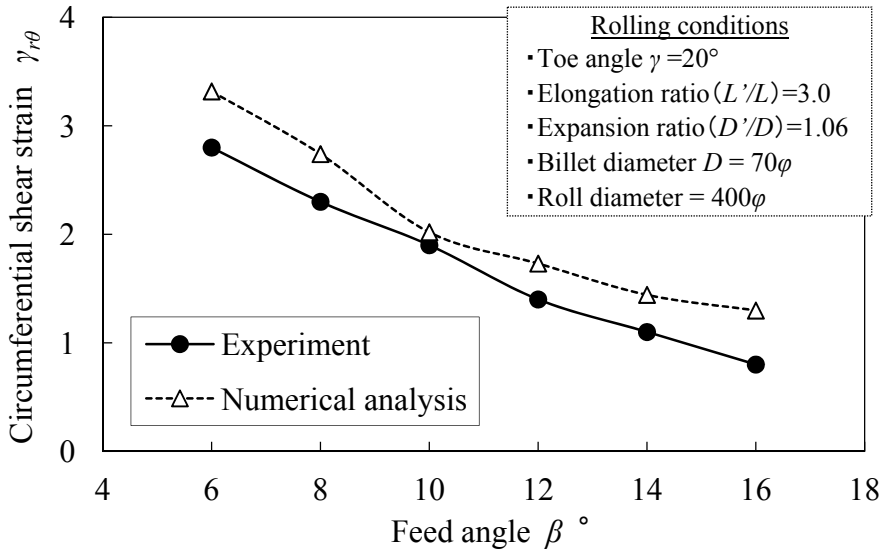

Figure 10: Effect of the feed angle β on circumferential shear strain $\gamma_{r\theta}$.

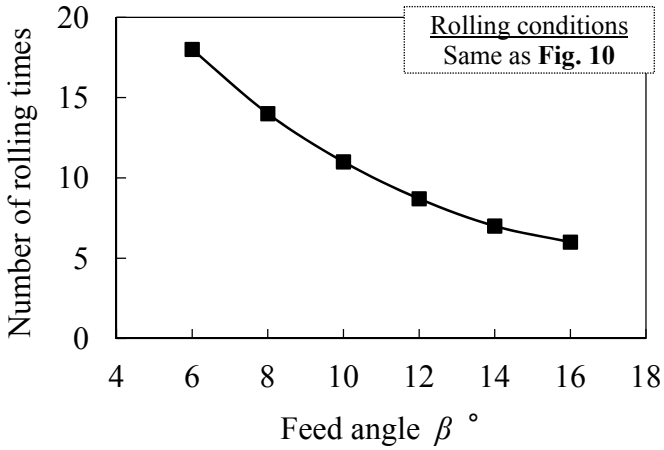

Figure 11: Effect of the feed angle β on the number of rolling times.

5 CONCLUSIONS

- The three-dimensional numerical analysis of the rotary piercing process was performed by the rigid plastic finite element method. The agreement of the numerical analysis results with the experimental results concerning circumferential shear strain $\gamma_{r\theta}$ confirms the validity of the developed numerical analysis model.
- The experiment and the numerical analysis clarified the effect of the toe angle γ and the feed angle β on circumferential shear strain $\gamma_{r\theta}$. As the toe angle γ or the feed angle β was increased, circumferential shear strain $\gamma_{r\theta}$ was suppressed. This paper clearly shows that the cone-type piercing mill with the high toe angle has an advantage of suppressing redundant shear deformation.

REFERENCES

[1] C.Hayashi and T.Yamakawa , Influences of Feed and Cross Angle on Rotary Forging Effects and Redundant Shear Deformation in Rotary Piercing Process , *ISIJ Int.* , (1997) **37**: 146-152.

[2] C.Hayashi and T.Yamakawa , Comparison of Double and Single Piercing Process in Seamless Steel Tube Manufacture , *Materials Science Research International* , (1997) **3**: 143-150.

[3] C.Hayashi and T.Yamakawa , Influences of Feed and Cross Angle on Inside Bore and Lamination Defects in Rotary Piercing for Materials with Poor Hot Workability, *ISIJ Int.* , (1997) **37**: 153-160.

[4] E.Erman , The influence of the processing parameters on the performance of the two-roll piercing operation , *Journal of Mechanical Working Technology* , (1987) **15**: 167-179.

[5] K.Mori , H.Yoshimura and K.Osakada , Simplified three-dimensional simulation of rotary piercing of seamless pipe by rigid-plastic finite-element method , *Journal of Materials Processing Technology* , (1998) , **80-81**: 700-706.

[6] R.Kawalla , E.Höfer , G.Lehmann and W.Lehnert , Use of finite element method for deeper analysis of rotary piercing , *Metal Forming 2000* , (2000) , 229-235.

[7] Hansgeorg Schoß , Nutzung der FEM beim Schrägwalzlochen , *Meform 2001 TU Bergakademie Freiberg* , (2001) , 317-331.

[8] E.Ceretti , C.Giardini , A.Attanasio , F.Brisotto and G.Capoferri , Rotary tube piercing study by FEM analysis: 3D simulations and experimental results , *Tube & Pipe Technology* , (2004) , 155-159.

[9] J.Pietsch and P.Thieven , FEM simulation of the rotary tube piercing process , *MPT International* , (2003) **26**: 52-60.

[10] K.Komori , Simulation of Mannesmann piercing process by the three-dimensional rigid-plastic finite-element method , *International Journal of Mechanical Sciences* , (2005) **47**: 1838-1853.

[11] Diego A.Berazategui , Miguel A.Cavaliere , Luca Montelatici and Eduardo N.Dvorkin , On the modelling of complex 3D bulk metal forming processes via the pseudo-concentrations technique. Application to the simulation of the Mannesmann piercing process , *Int. J. Numer. Meth. Engng* , (2006) **65**: 1113-1144.

[12] Z.Pater , J.Kazanecki and J.Bartnicki , Three dimensional thermo-mechanical simulation of the tube forming process in Diescher's mill , *Journal of Materials Processing Technology* , (2006) **177**: 167-170.

[13] R.Pschera , J.Klarner and C.Sommitsch , Finite-Elemente-Modellierung des Schrägwalzens , *Berg- und Hüttenmännische Monatshefte* , (2007) **152**: 205-211.

[14] A.Ghiotti , S.Fanini , S.Bruschi and P.F.Bariani , Modelling of the Mannesmann effect , *CIRP Annals – Manufacturing Technology* , (2009) **58**: 255-258.

[15] K.Komori and K.Mizuno , Study on plastic deformation in cone-type rotary piercing process using model piercing mill for modeling clay , *Journal of Materials Processing Technology* , (2009) **209**: 4994-5001.

[16] R.Krux and M.Zemko , FEM-modelling of Barrel-type Cross-roll Piercing and Analysis of the Induced Rotational Motion of the Plug Bar , *ICTP* , (2011) , 143-148.

[17] Z.Pater and J.Kazanecki , Complex Numerical Analysis of the Tube Forming Process Using Diescher Mill , *Archives of Metallurgy and Materials* , (2013) **58**: 717-724.